



PII S0008-8846(96)00093-2

CRACK ARREST IN MORTAR MATRIX REINFORCED WITH UNIDIRECTIONALLY ALIGNED FIBERS

Mohsen A. Issa

Associate Professor, Department of Civil and Materials Engineering
University of Illinois at Chicago, Chicago, Illinois 60607

A.B. Shafiq

Research Associate, Department of Civil and Materials Engineering
University of Illinois at Chicago, Chicago, Illinois 60607

Ahmad M. Hammad

Visiting Lecturer & Structural Engineer
T. Y. Lin International-Bascom, Chicago, Illinois 60646

(Refereed)

(Received October 12, 1995; in final form May 13, 1996)

ABSTRACT

This paper presents an investigation on the effects of reinforcement size, reinforcement spacing and specimen size on the fracture parameters of notched mortar specimens reinforced with long aligned steel fibers. A total of 33 specimens of variable fiber size, fiber spacing and specimen size were tested under quasi-static monotonic and cyclic loading conditions. For a constant volume fraction of steel reinforcement, the experimental results indicate an increase in the fracture energy as the size of the reinforcing fibers and the corresponding spacing between the fibers is reduced. Finite element analysis indicates that the closing pressures imposed by the bridging of the fibers in the wake of the crack-tip increase as the spacing between the fibers is decreased, particularly as the spacing approaches approximately 6.25 mm. Within the testing range, the fracture energy (G_F), energy release rate (G_{Ic}) and stress intensity factor (K_{Ic}) appear to be independent of the specimen thickness.

Introduction

Cracking in concrete usually takes place due to randomly distributed flaws inherent in its nature. These randomly distributed micro-cracks coalesce under service conditions forming macro-cracks and lead to the catastrophic failure of the structure. Therefore, concrete is generally reinforced with a form of continuous or randomly distributed steel fibers and bars. These fibers inhibit crack initiation and growth, hence increasing the fracture toughness of concrete. Literature on the experimental evaluation of fracture behavior in concrete reinforced with long aligned fibers is scarce, and there is conflicting scatter present in the reported results.

Romualdi and Batson [1,2] concluded that an increase in tensile cracking is proportional to the inverse square root of the fiber spacing, however, the influence is not pronounced until the spacing between the fibers approaches approximately 7.5 mm. Shah and Rangan [3] experimentally observed a slight influence of fiber spacing on crack propagation when the fiber spacing was reduced below 25 mm. For a brittle matrix, Kelly [4] predicted the dependency of the failure strain (ϵ) on fiber spacing “R” and fiber radius “r” as:

$$\epsilon \propto \frac{r a^{3/2}}{R^{4/3} V_m} \quad (1)$$

where “ V_m ” is the volume fraction of the matrix and “a” is a constant that depends on the geometry of the array. According to ACK’s model, the mechanical properties are independent of the size of the reinforcement whereas, an increase in the work of fracture is possible when the size of the reinforcement increases or when there is an increase in the fiber matrix bond.

Hillerborg *et al.* [5,6] analyzed the fibers crossing the crack using the fictitious crack model and found that fracture energy is fiber size independent. According to Marshall *et al.* [7,8], an increase in fiber size or fiber strength results in an increase in fracture toughness of the composite. Mura *et al.* [9] based on the inclusion model showed that the presence of the supporting fibers reduces the values of K_{Ic} and G_{Ic} which saturate at a certain level according to the optimum size and spacing of the fibers. The dependence of fiber size and spacing on the stress intensity factor is given as:

$$K = K_o \frac{\left(1 + \frac{2}{3} \pi ar/\lambda^2\right)^{1/2}}{(1 + \pi ar/\lambda^2)} \quad (2)$$

where “ K_o ” is the stress intensity factor of the crack without the fibers and “a”, “r” and “ λ ” are the crack length, fiber radius and fiber spacing, respectively.

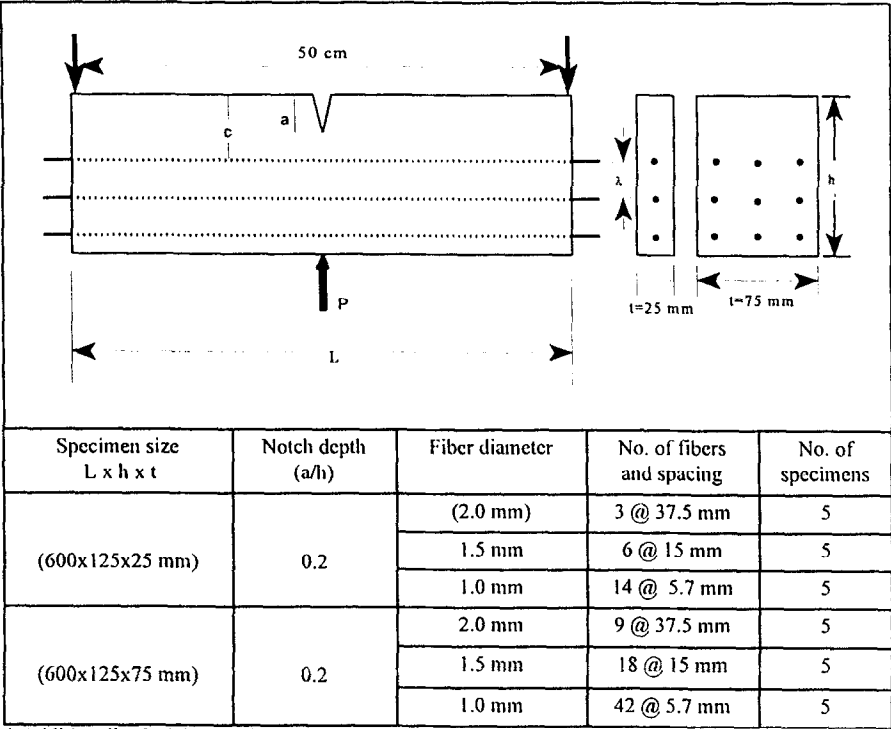
Research Significance

Most structural designs are based on ultimate loading conditions. It is known that slow crack growth starts long before the concrete reaches its ultimate stress. To account for this phenomena in design, fracture parameters provide an insight into how a material behaves under pre-ultimate service loads. It is imperative to comprehend the nature of the parameters that have a direct influence on the integrity and the lifetime of structures designed using these composites. The present research undertakes this task by studying the effect of reinforcement size, corresponding spacing between fibers and specimen size in concrete reinforced with long aligned fibers.

Experimental Program

Thirty three specimens of varying thickness, number and spacing of fibers were tested under 3-point bending loading condition. The percentage of steel reinforcement was kept constant in all specimens, and the specimens were designed such that the fibers yielded prior to concrete crushing. Table I summarizes the specimen dimensions, matrix and fiber properties. The first

TABLE 1
Summary of Material Properties and Specimen Geometry



* Additionally, 3 plain (unreinforced) specimens of 25 mm thickness were tested.

fiber was placed at 12.5 mm from the notch tip. Type I Portland cement and river sand with a maximum aggregate size of 4.6 mm were used. The mix proportions by weight were water: cement:sand = 0.4:1.0:2.0. The specimens were fabricated in a plexiglass mold and then unmolded and cured for 14 days in 100% relative humidity. The average compressive strength of the matrix was 51.7 MPa and the direct tensile strength was 4.48 MPa. The yield strength of the steel reinforcing fibers was 380 MPa.

A servo-hydraulic Instron machine equipped with a digital controller, was used to test the mortar composite specimens. All readings from the COD extensometer, load cell and LVDT were recorded by a data acquisition system. Testing was performed in three-point bending displacement control mode at a constant rate of loading of 0.075 mm/min. The rate of loading and unloading was kept constant. The specimens were loaded until the crack propagated, at which point the loading was immediately switched to unloading. After complete unloading, the specimens were reloaded and the same procedure was repeated until the crack traveled through the entire depth of the specimen. Static, monotonic tests were also performed to obtain load-CMOD curves to investigate the influence of fiber size and spacing on the mechanical properties of mortar composites.

Crack Length Measurement

Crack length measurement in concrete has always been a subject of great difficulty and controversy. Surface measured crack lengths have been shown to be erroneous due to the parabolic crack front in concrete, unequal crack lengths on either side of the specimen and inconsistencies in the crack length measuring techniques, thus rendering the analysis based on these crack lengths feeble. In the absence of the surface measured crack lengths, researchers have relied on the estimated crack lengths which are generally based on LEFM. A great deal of controversy exists over applying LEFM to concrete and it has been shown by Hillerborg [7,8,10] and several other researchers that LEFM cannot be applied to concrete and especially to fiber reinforced concrete. Therefore, any estimate of the crack length based on LEFM leads to inaccurate results.

Any estimate of crack length based on LEFM yields an exponential curve. Fig. 1a depicts typical empirical plots of CMOD versus crack length based on the LEFM. Only in a small a/h range, physically acceptable crack lengths can be observed. As a/w increases, the crack length increments get smaller whereas experimental CMOD increments during successive cycles remain almost the same, which is physically unrealistic and unacceptable. For any kind of cementitious material subjected to cyclic loading, the energy required to propagate the matrix crack decreases as the crack length increases. LEFM obtained crack lengths suggest an increase in the energy absorption as the crack grows for plain concrete. Fig. 1b compares typical plots of fracture energy versus the crack length increment based on compliance method crack lengths, surface measured crack lengths and crack lengths calculated using the proposed method in this study.

The authors feel that there has to be a realistically obtained crack length which is consistent with the physics of the material. In the present study, a very simple method of estimating the crack length is employed. It is based on the assumption that COD is linearly proportional to the

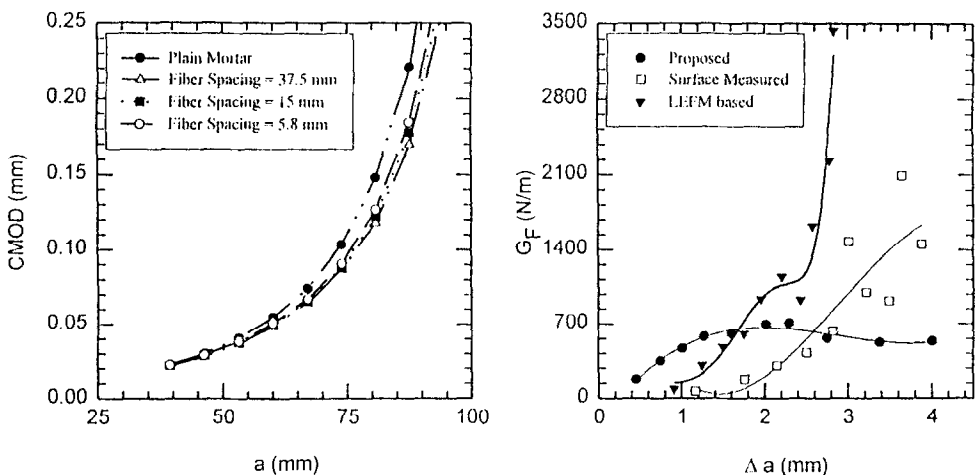


FIG. 1.

(a) Typical LEFM based CMOD versus crack length for various specimens tested, (b) Fracture energy versus incremental crack length.

crack length. It is a realistic assumption for quasi-brittle materials like concrete where there is negligible deformation and stretching in the matrix in the vicinity of the crack-tip and no appreciable deformation in the crack profile in the wake of the crack-tip. It is further assumed that the crack propagates when there is a change in the slope of the ascending curve and crack propagation stops when COD starts decreasing at the beginning of the descending curve of each cycle. At the end of the test, the crack is assumed to have penetrated through the entire depth of the specimen. A crack length is obtained at the end of each cycle by relating the specimen depth to the maximum COD at complete specimen failure.

$$\frac{\text{total COD}}{\text{depth of specimen}} = \frac{\text{maximum COD in a particular cycle}}{\text{crack length at that cycle}} \quad (3)$$

Following this technique, physically acceptable fracture energies were obtained that matched the fracture behavior of such materials. A detailed discussion of fracture results is provided in the following sections.

This procedure can only be used to obtain the crack lengths at the end of each cycle. Crack lengths obtained at random locations of the loading-unloading curves would be incorrect. At the end of each cycle, when the loading has switched to unloading, the crack propagation stops and this is the point where the crack lengths should be measured for a particular cycle and not at the ultimate loads. This procedure has to be repeated for each test. Calibration tests would not work due to the fact that for each test, the maximum COD varies and loading-unloading curves are different.

Mechanical Behavior

The ultimate strength of plain concrete was about 20% lower than that of the reinforced mortar specimens. The pre-cracking behavior of plain and fiber reinforced specimens was independent of the fiber size, spacing between the fibers and specimen size. However, the post-cracking behavior exhibited a dependence on the fiber size and spacing between the fibers. A sharp decrease in the load was observed as the crack propagated in the plain mortar specimens. For the fiber reinforced specimens, as the crack propagated through the first fiber, load was partially transferred to the fiber. When the crack propagated further and passed through additional fibers, the load transferred to subsequent fibers. As the load was transferred to the fibers, the descending part of the load-deflection curve stabilized (Fig. 2). The post-cracking toughness of the material increased with an increasing number of fibers. Although the volume fraction of steel was kept constant, the load transfer mechanism was different. As the number of fibers increased, the stress localization decreased, resulting in an improved toughness and post-cracking strength of the material.

Fracture Energy (G_F)

The mechanical strength is based on the undamaged material, while the fracture strength depends on the interlocking of the fracture surface, crack bridging and strength and stiffness of the concrete and reinforcement. At peak loads, the stress transfer capability depends on the strength and stiffness of the constituents that comprise the specimen. If the matrix is stronger

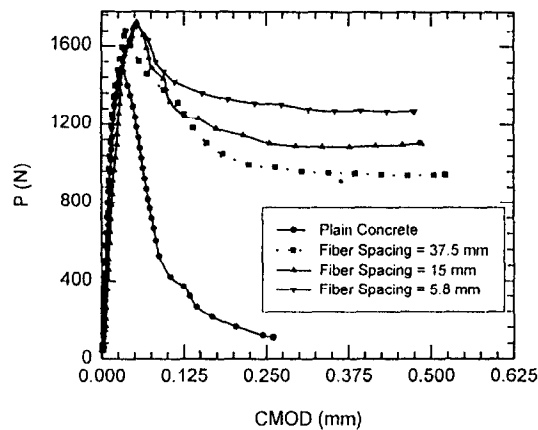


FIG. 2.

Typical experimental load versus CMOD curves for specimen thickness of 25 mm.

than the fibers, the stresses in the composite decrease as the crack propagates, whereas, if the reinforcing fibers are stronger than the matrix, the stress in the composite increases. The specimens tested in this study are of the latter type; the steel reinforcement is an order of magnitude stronger than the matrix.

Fracture energy is a critical material property as it is the materials' resistance to crack growth. Fracture energy was determined from the loading-unloading technique described earlier and was calculated as:

$$G_F = \frac{W_o}{A_{lig}} \quad (4)$$

where " W_o " is the strain energy release rate obtained from the area under the load-CMOD diagram, and " A_{lig} " is the area of the cracked ligament. Average values along with the standard deviation of fracture energies of different specimens are plotted against the crack advance (Δ) in Figs. 3a and 3b. The matrix cracked at approximately the same failure strain for both plain and reinforced specimens before bridging of the fibers took effect, resulting in similar initial fracture energy values. An increase in fracture energy was observed as the number of fibers in the wake of the crack-tip increased. The smaller spacing between the fibers and the greater number of fibers result in an increase in fracture energy as the crack propagates. This increase in fracture energy can be attributed to the increased surface area, better bond and increased stress transfer capability. As the crack grew, G_F for plain mortar decreased whereas the G_F in the fiber reinforced concrete kept increasing until most of the stresses were transferred from the matrix to the fibers and the composite action of the matrix and fibers was no longer effective. Fracture energy had a decreasing trend once the stresses were transferred to the fibers.

It is apparent that there is an increasing and then a decreasing trend in the fracture toughness values. The effect producing an increase in the fracture toughness may be attributed to an increase in the size of the micro-cracking zone. Larger crack lengths result in larger areas affected by damage accumulation. Since the introduction of micro-cracks surrounding the main crack-tip blunts the effects of high stresses, the amount of energy required to produce failure

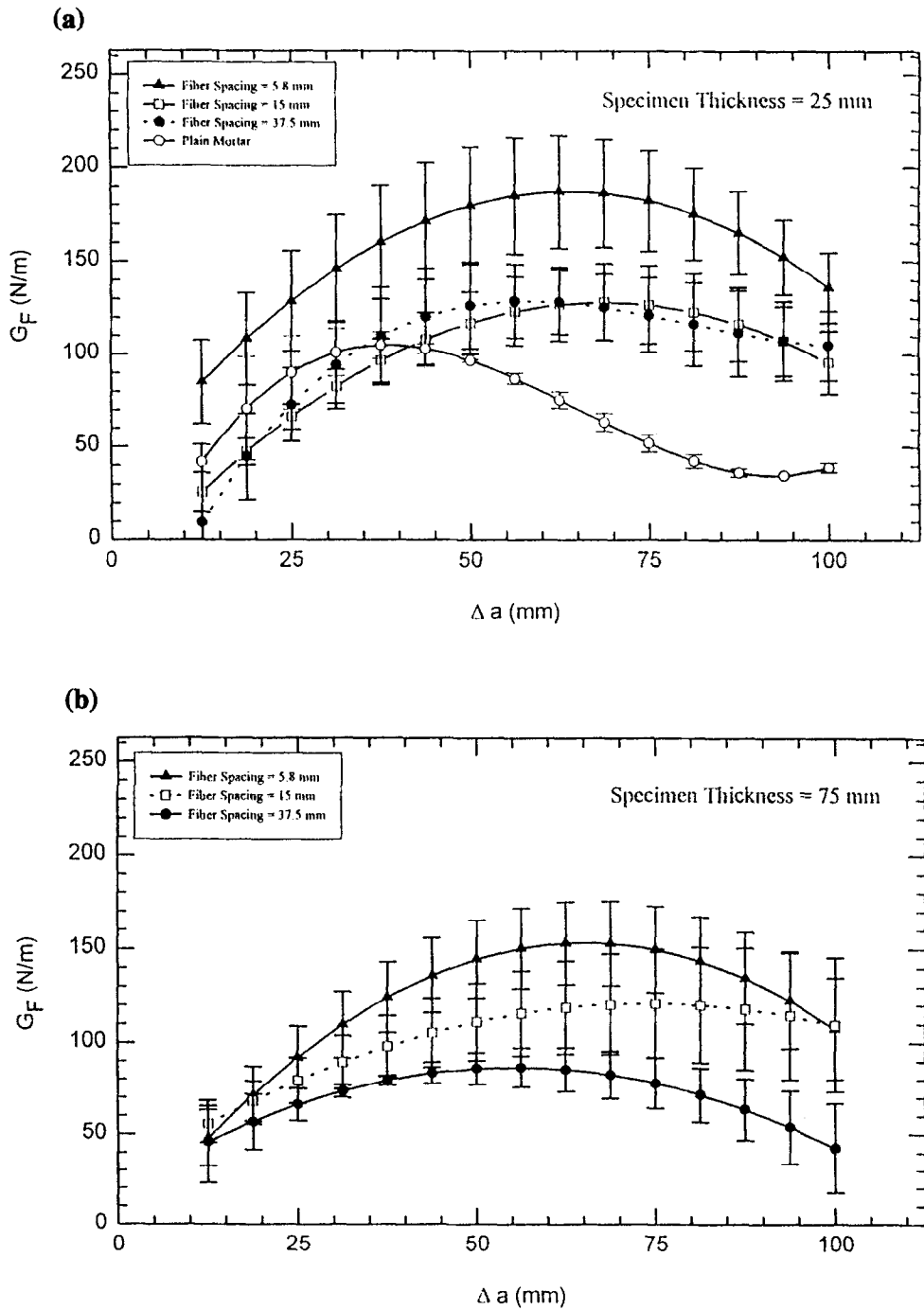


FIG. 3a and 3b.

Average values along with standard deviations of fracture energy as a function of crack advance for different specimen thicknesses.

is increased. A larger area of micro-damage results in an increase in the fracture toughness. The phenomenon of micro-damage shielding the main crack from propagation has been observed by [10,11,12] in other materials.

The effect of a parabolic trend of fracture energy may also be associated with the heterogeneous nature of reinforced concrete. The number of micro-cracks that must be coalesced to produce failure is related to the size of the uncracked ligament. With a decreasing uncracked ligament, the number of possible weak crack paths that could produce failure decreases, however, the probability of failure increases much faster. Therefore, the total probability of failure increases resulting in a decreased fracture toughness.

Among the several factors that influence the increase in fracture energy, the stress transfer capability plays an important role. By increasing the number of fibers due to a reduction in the fiber diameter, the stress transfer capability between the fibers and the matrix can be improved. For a crack length of just under 37.5 mm, the crack in the 14 fiber specimen is bridged by five fibers of 1 mm diameter as opposed to crack bridging by 1 fiber of 2 mm diameter in the 3 fiber specimen. Therefore, the crack arrest mechanism is more effectively controlled if the spacing between the fibers is reduced for the same percentage of steel reinforcement.

The average G_F values given in Figs. 3a and 3b for the three and six fiber specimens were generally within 15% of each other, whereas, G_F values for the 14 fiber specimens were 25% - 40% higher than the 3 or 6 fiber specimens. In some cases, a 100% increase in G_F between the 3 and 14 fiber specimens was observed. In general, fracture energy increased as the number of fibers increased, however, there seems to be a threshold range below which the influence is not well pronounced. Similar results have been reported by Romualdi and Batson [1,2] who concluded that the effect of reinforcement is not significant until the fiber spacing reduces to approximately 7.5 mm. Their theoretical results show that by reducing the spacing from 25 mm to 2.5 mm, the strength increases by more than 300%, while the experimentally observed increase in strength by [3] was less than 25% following similar testing. Shah and Rangan [3] concluded that the effect of spacing effect is insignificant below a fiber spacing of 25 mm.

Stress Intensity Factor and Energy Release Rate

Calculation of K_{Ic} and G_{Ic} based on LEFM represents only the energy consumed in crack initiation, ignoring the energy spent on crack growth and formation of micro-cracks, whereas, G_F takes into account the total energy consumption, i.e., the entire area under the load-CMOD curve. Measurement of K_{Ic} and G_{Ic} , especially at small crack growths may provide useful data on the toughness of the composite before the load is carried entirely by the fibers. The stress intensity factor, K_{Ic} , was calculated using LEFM. The total stress intensity factor was obtained as:

$$K_{total} = K_{remote} + \sum K_{bridging} \quad (5)$$

where “ K_{remote} ” is the stress intensity factor due to the externally applied load and “ $K_{bridging}$ ” is the stress intensity factor due to the closing pressures of the bridging fibers in the wake of the crack-tip. K_{remote} can be obtained from:

$$K_{remote} = \frac{3LP_{remote}}{2h^2t} \left[1.09 - 1.735 \left(\frac{a}{h} \right) + 8.2 \left(\frac{a}{h} \right)^2 - 14.18 \left(\frac{a}{h} \right)^3 + 14.57 \left(\frac{a}{h} \right)^4 \right] \quad (6)$$

and K_{bridging} can be calculated form:

$$K_{\text{bridging}} = \frac{2P_{\text{bridging}}}{t\sqrt{\pi a}} \left[\frac{3.52(1 - c/a)}{(1 - a/h)^{3/2}} - \frac{4.35 - 5.28c/a}{(1 - a/h)^{1/2}} \right] + \frac{2P_{\text{bridging}}}{t\sqrt{\pi a}} \left[\left(\frac{1.3 - 0.3(c/a)^{3/2}}{\sqrt{1 - (c/a)^2}} + 0.83 - 1.76c/a \right) (1 - (1 - c/a)a/h) \right] \quad (7)$$

Since there is no closed form solution available to account for the closing pressure of the fibers, several schemes [7,13] are suggested for its approximation. In this study, finite element analysis was employed to determine the closing pressures. The results of the sum of the fiber closing pressures at varying crack lengths are given in Fig. 4a. The fiber closing stresses for the fibers of spacing 37.5 and 15 mm were within 70% of each other, whereas, the closing pressures for the specimens with 6.25 mm spacing increased by approximately 250%. However, this increase in the closing pressures does not produce a significant increase in K_{Ic} since the overall increase in the closing forces was within 20%. Up to a 72% reduction in the stress intensity was observed due to the closing pressures of the fibers in the wake of the crack-tip. The Experimentally obtained crack-tip stress intensity was independent of the size and spacing of the fibers (Fig. 4b). Romualdi and Batson [1] and Chang and Chai [13] observed an increase in the cracking stresses with a decrease in fiber spacing. K_{Ic} and G_{Ic} , according to the inclusion model [9] increase as the fiber spacing is increased as shown in Fig. 5. LEFM based K_{Ic} appears to be independent of the fiber spacing whereas K_{IM} strongly depends on the spacing between the fibers. Figs. 5b, 5c and 5d compare G_{F} with G_{Ic} (based on LEFM) and G_{IM} (based on inclusion model) for specimens with variable spacing between the fibers. G_{IM} matches more closely to

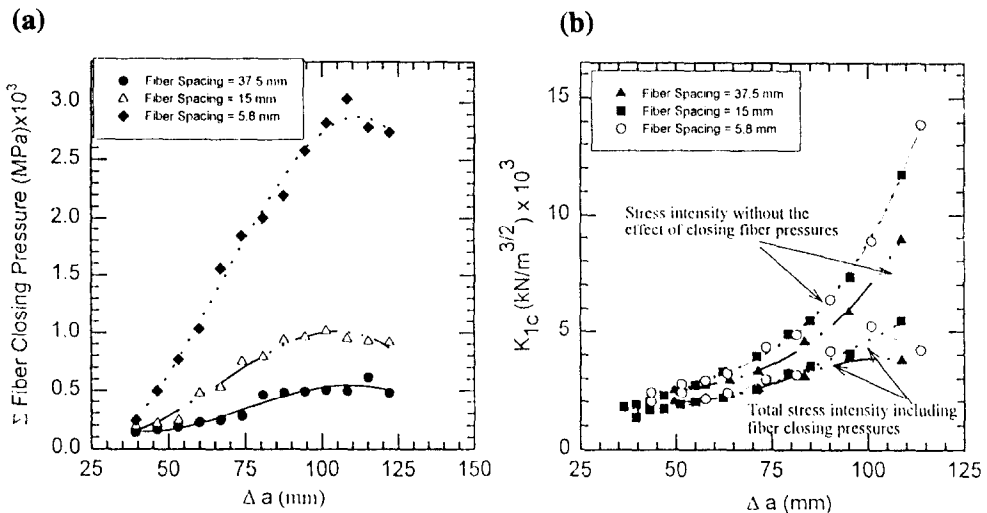


FIG. 4.

(a) Sum of fiber closing pressures as a function of incremental crack length for specimens with variable fiber spacing, (b) stress intensity factor as a function of crack advance with and without fiber closing pressures.

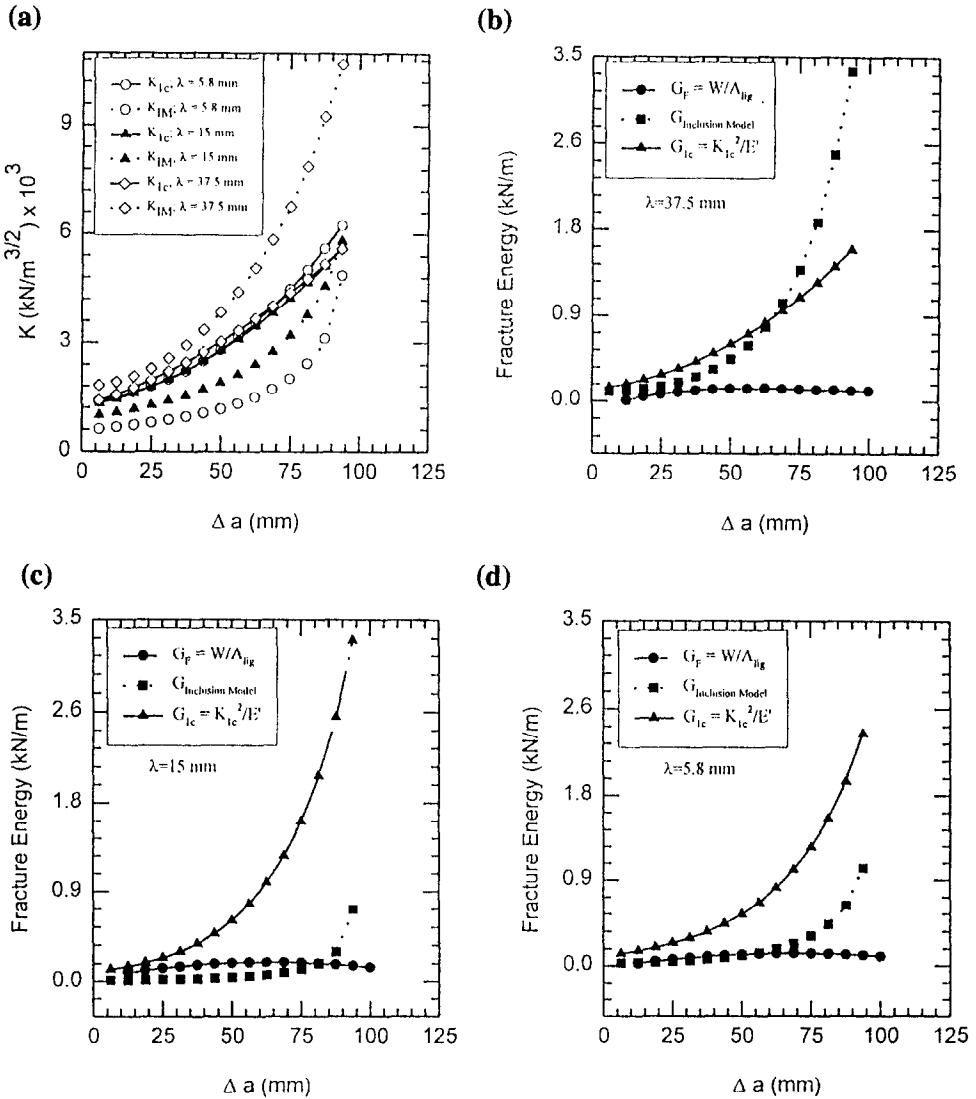


FIG. 5.

(a) Average values of K_{Ic} and K_{IM} for specimens with variable fiber spacings, (b,c,d) average values of G_F , G_{Ic} and G_{IM} for specimens with fiber spacings of λ , 37.5, 15 and 5.8 mm, respectively.

the G_F for the fiber spacing (λ) < 25 mm as shown in Figs. 5c and 5d, whereas for $\lambda > 25$ mm (Fig. 5b), a significant deviation from experimentally observed G_F is observed.

Size Effect

Results of the present study indicate that the flexural toughness, fracture energy, energy release rate and stress intensity factor are independent of the specimen thickness at all levels of fiber

size, fiber spacing and specimen thickness. The size effect on concrete strength primarily results from strain localization at failure. It has been shown that with an increase in reinforcement, the effect of the strain localization can be reduced.

Unlike metals, micro cracking in concrete is not accompanied by any substantial contraction. As a result, the width of the specimen may not be of major importance for concrete composites. The experimental results support this analysis as all fracture parameters appear to be independent of the specimen thickness. Similar results have been reported by Bressi [14]. A comparison of G_F between 25 and 75 mm thick specimens can be made from Fig. 3. Seventy five millimeters (75 mm) thick specimens bear a keen similarity to the trend observed in the comparable 25 mm thick specimens. The values of G_F for specimens with fiber spacings of 37.5 and 15 mm were within experimental error for both 25 mm and 75 mm thick specimens, whereas G_F for a fiber spacing of 5.8 mm was 25-40 % higher in both cases. Mindess [15] increased the size three times and found very little influence of specimen size on the fracture toughness of the material. Results of the present testing are also in accordance with Ouyang and Shah's [16] analysis, the volume fraction of 0.04 used in the present case was the upper limit in their analysis where they observed an insignificant influence of specimen size on the strength and toughness of the material.

The mechanical properties also appear to be independent of the specimen thickness. The load-CMOD curves of comparable 25 and 75 mm thick specimens were observed to have similar trends. The compliance and strain to failure were approximately the same for the different specimens. For the 75 mm thick specimen, the ultimate load was approximately three times that of the 25 mm thick specimens. Chen et al. [17] observed a decrease of 7% in the ultimate strength when the width of the specimen was increased 3 folds in the steel fiber reinforced concrete specimens.

Summary and Conclusions

The phenomenon of slow crack growth in fiber reinforced mortar prior to peak loading conditions warrants a need to understand the factors influencing this behavior. Fracture energy, stress intensity factor and energy release rate are some of the most important parameters that yield information in regard to the fracture behavior of a material. An experimental program was conducted to examine the effects of reinforcement size, reinforcement spacing and specimen size on the fracture behavior of concrete reinforced with long aligned fibers. The conclusions may be summarized as follows:

1. Increasing the fiber size or the corresponding spacing between the fibers decreases the fracture energy of the mortar reinforced with long aligned fibers. An increase in fracture energy with respect to the fiber spacing is gradual, however, it is not significant until the spacing is reduced to 6.35 mm.
2. Experimental results suggest that stress intensity factor is not influenced by the size of the fibers or fiber spacing.
3. Closing pressures imposed by the bridging of the fibers increase as the size and the corresponding spacing between the fibers is reduced. The effect is more pronounced as the spacing is reduced to approximately 6.35 mm.
4. Fracture energy, energy release rate and stress intensity factor are independent of the thickness of the specimen.

References

1. Romualdi, J. and Batson, G., "Mechanics of Crack Arrest in Concrete," *J. Eng. Mech.*, pp. 147-168, June 1963.
2. Romualdi, J. and Batson, G., "Behavior of reinforced concrete beams with closely spaced reinforcement," *J. Am. Conc. Inst.*, pp. 775-789, June 1963.
3. Shah, S. and Rangan, V., "Fiber Reinforced Concrete Properties," *J. Am. Conc. Inst.*, V. 68, pp. 126-135, 1971.
4. Kelly, A., "Microstructural parameters of an aligned fibrous composite," Conference on the Properties of Fiber Composites, National Physical Laboratory, pp. 5-14, 1971.
5. Hillerborg, A., Modeer, M. and Peterson, P., "Analysis of crack formation and crack growth in concrete by means of fracture mechanics and finite elements," *Cem. Conc. Res.*, V. 6, pp. 773-782, 1976.
6. Hillerborg, A., "Analysis of fracture by means of the fictitious crack model, particularly for fibre reinforced concrete," *Int. J. Cem. Comp.*, V. 2, pp. 177-184, 1980.
7. Marshall, B.; Cox, B.; and Evans, A., "The mechanics of matrix cracking in brittle-matrix fiber composites," *Acta Meta.*, V. 30, n. 11, pp. 2013-2021, 1985.
8. Marshall, D. and Cox, B., "Tensile fracture of brittle matrix composites: Influence of fiber strength," *Acta. Meta.*, V. 35, N. 11, pp. 2607-2619, 1987.
9. Mori, T. and Mura, T., "An inclusion model for crack arrest in fiber reinforced materials," *Mech. Mat.*, V. 3, pp. 193-198, 1984.
10. Peterson, P., "Fracture energy of concrete: Method of determination," *Cem. Conc. Res.*, V. 10, pp. 79-89, 1980.
11. Perdikaris, P.; Calmino, A.; and Chudnovsky, A., "Effect of fatigue on fracture toughness of concrete," *ASCE J. Eng. Mech.*, V. 112, N. 8, pp. 776-791, 1986.
12. Cedolin, L.; Poli, S.; and Lori, J., "Experimental determination of the fracture process zone in concrete," *Cem. Conc. Res.*, V. 13, pp. 557-567, 1983.
13. Chang, D. and Chai, W., "Flexural fracture and fatigue behavior of steel-fiber-reinforced concrete structures," *Nuc. Eng. Des.*, V. 156, pp. 201-207, 1995.
14. Bressi, D. and Ferrara, G., "Experimental and numerical determination of K_{Ic} and G_{Ic} for micro-concrete," *Proc. 5th Int. Con. Frac.* Cannes, France. V. 5, pp. 2719-2726, 1980.
15. Mindess, S., "The effect of specimen size on the fracture energy of concrete," *Cem. Conc. Res.*, V. 14, pp. 431-436, 1984.
16. Ouyang, C. and Shah, S., "Fracture energy approach for predicting cracking of reinforced concrete tensile members," *ACI Struc. J.*, V. 91, No. 1, 1994, pp. 69-78.
17. Chen, L.; Mindess, S.; and Morgan, D., "Specimen geometry and toughness of steel-fiber -reinforced concrete," *J. Mater. in Civil Eng.*, V. 6, N. 4, 1994, pp. 529-541.